

Supporting Information

Spin state engineered $\text{Zn}_x\text{Co}_{3-x}\text{O}_4$ as efficient oxygen evolution electrocatalyst

*Rani Mohan Ramsundar,^{a,c} Vijayamohanan Kunjukrishna Pillai^{b,c} and Pattayil Alias Joy *^{a,c}*

^aPhysical and Materials Chemistry Division, CSIR-National Chemical Laboratory, Pune 411008, India

^bCSIR-Central Electrochemical Research Institute, Karaikudi 630006, India

^cAcademy of Scientific and Innovative Research (AcSIR), Ghaziabad 201002, India

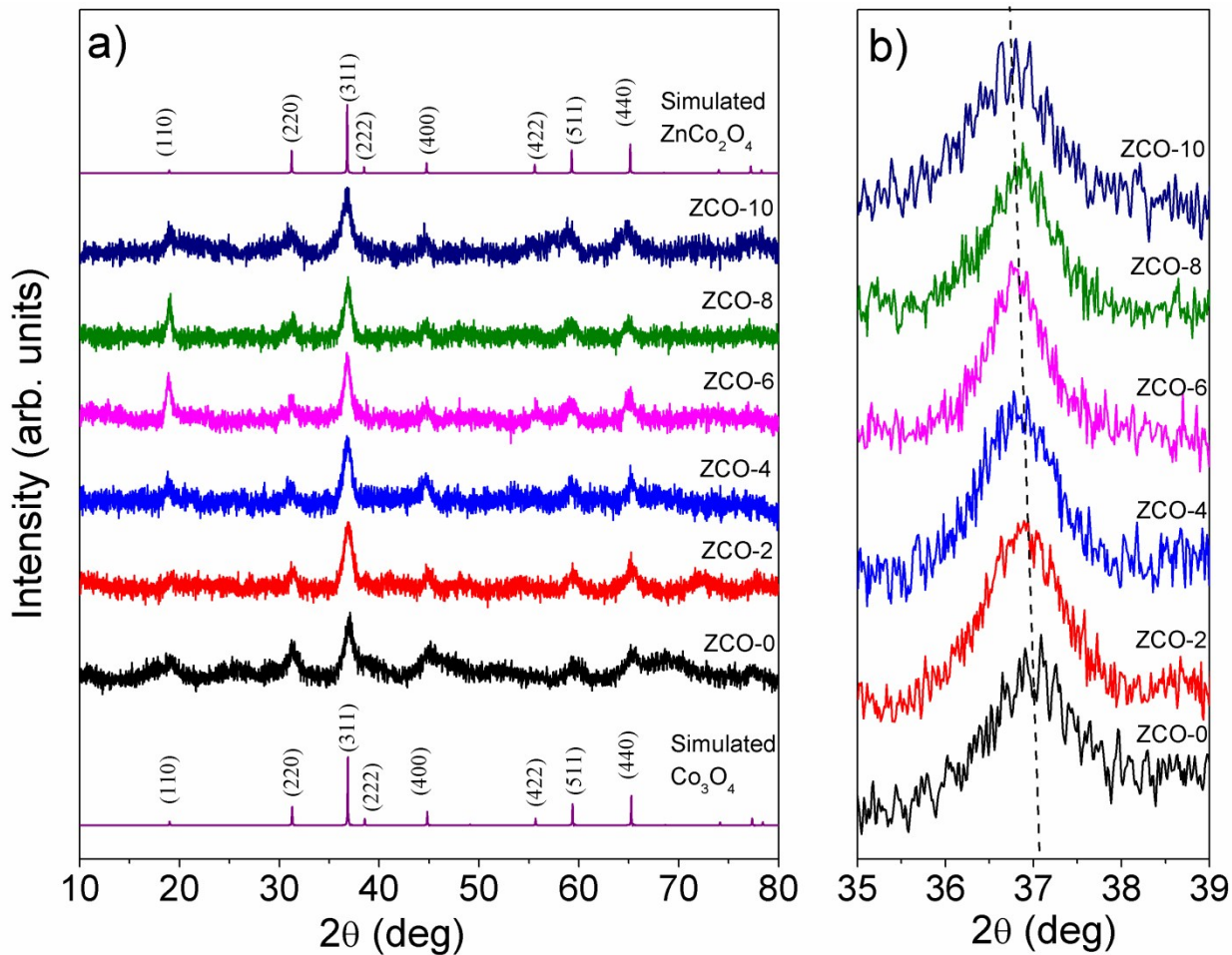


Fig. S1. (a) XRD patterns of the unsubstituted and Zn-substituted cobalt oxide compositions compared with the simulated patterns of the end members, and (b) magnified view of the (311) peak in the XRD patterns. The broken line in (b) indicates the small shift in the position of the peak to lower angles.

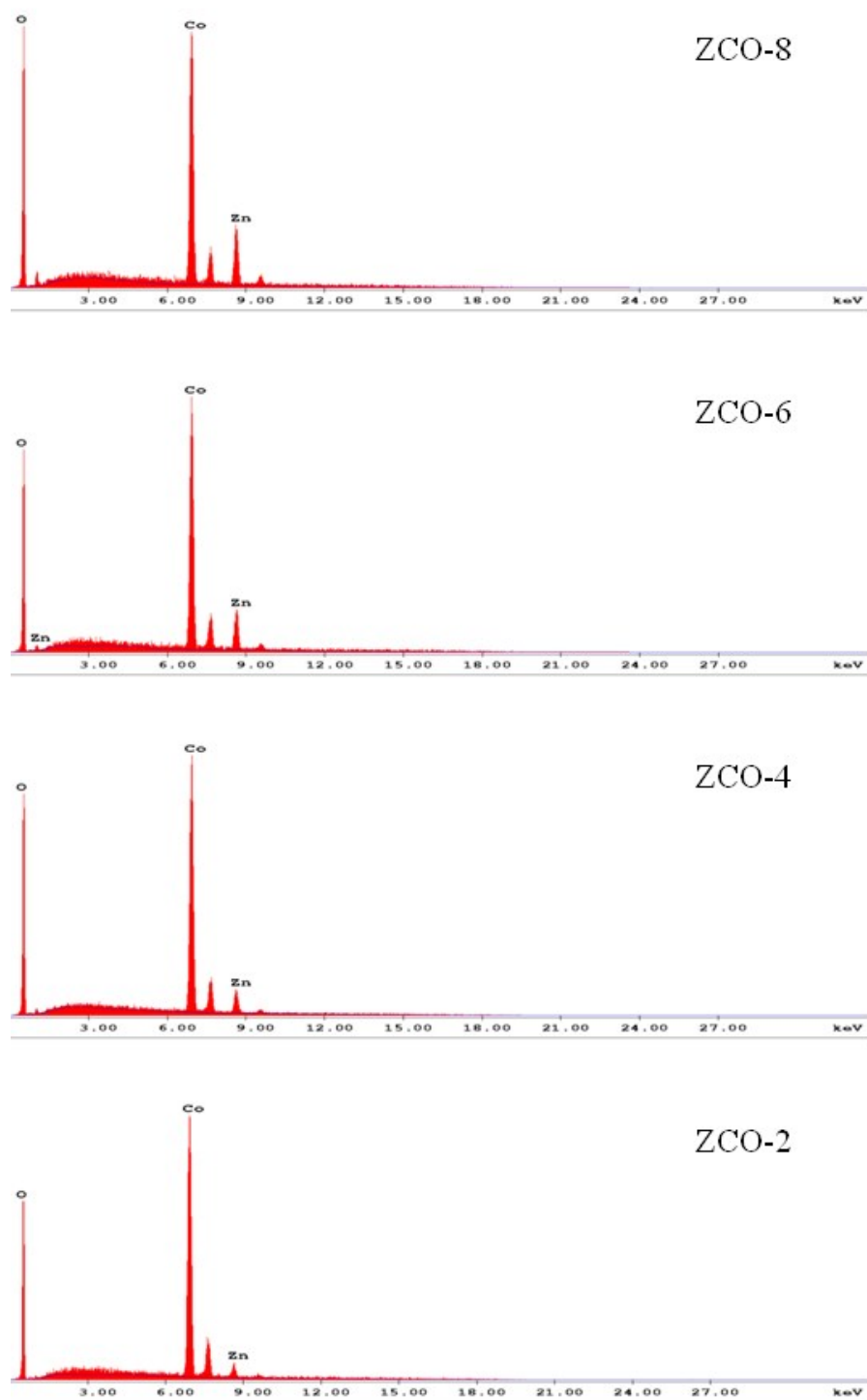


Fig. S2. EDX data of different compositions in $Zn_xCo_{3-x}O_4$

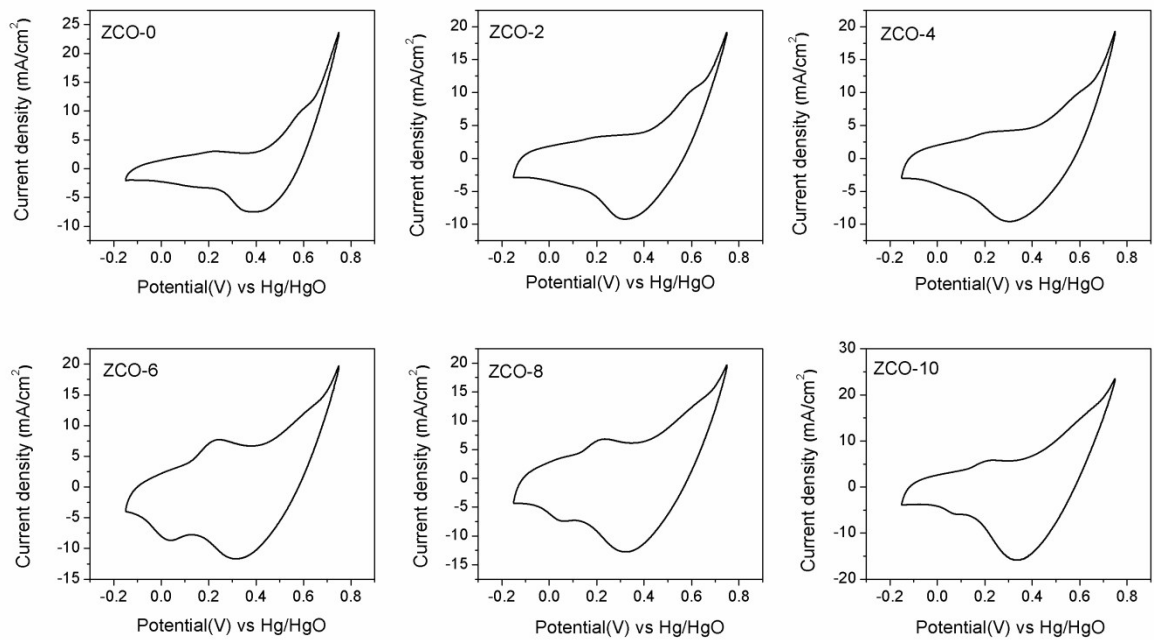


Fig. S3. Cyclic voltammetry curves of Zn_xCo_{3-x}O₄ in 0.1 M KOH, recorded at the scan rate of 50 mV/s

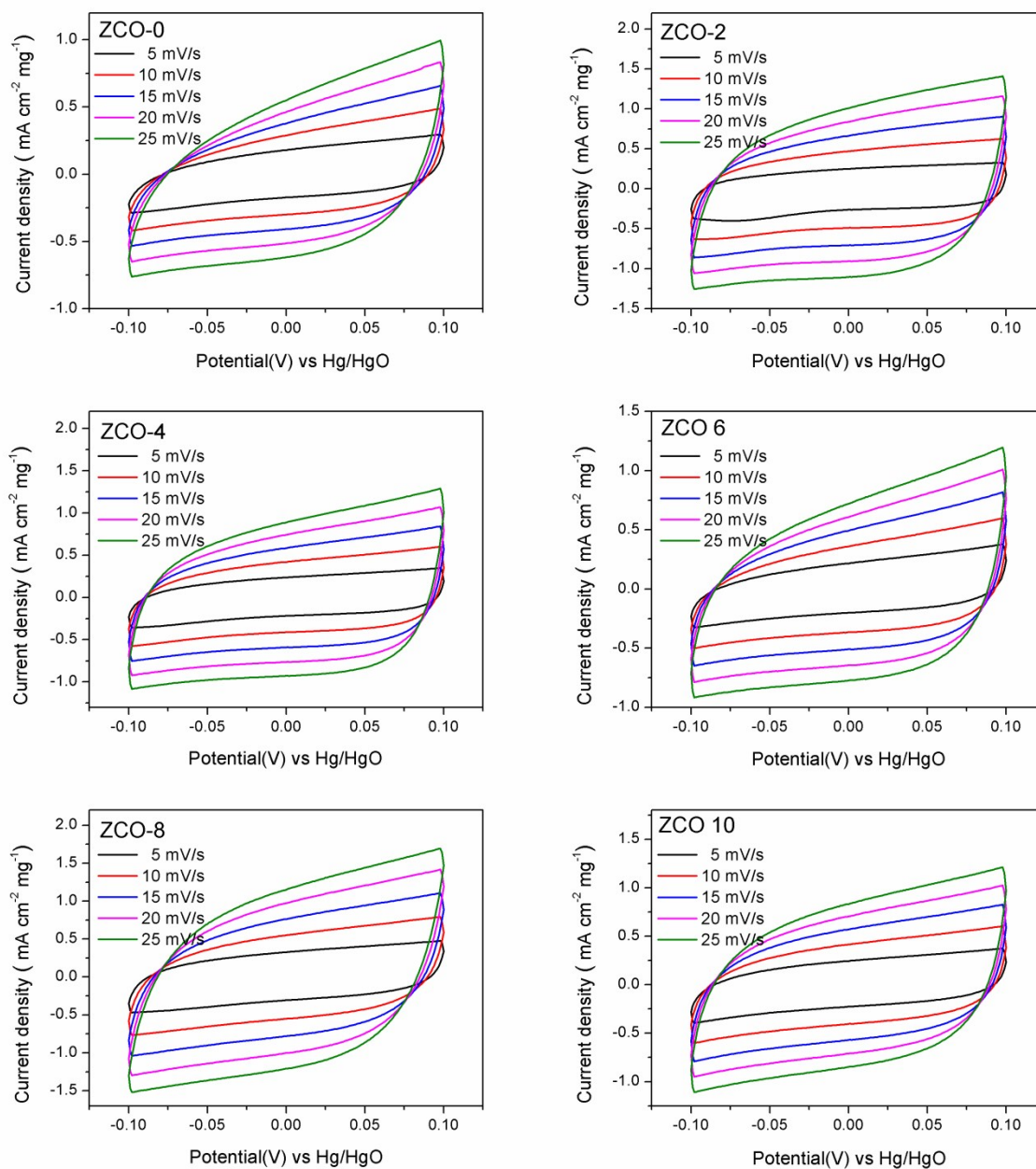


Fig. S4. Cyclic voltammety curves of $\text{Zn}_x\text{Co}_{3-x}\text{O}_4$ in 0.1 M KOH at different scan rates in the non-Faradic potential window (-0.1 to 0.1 V)

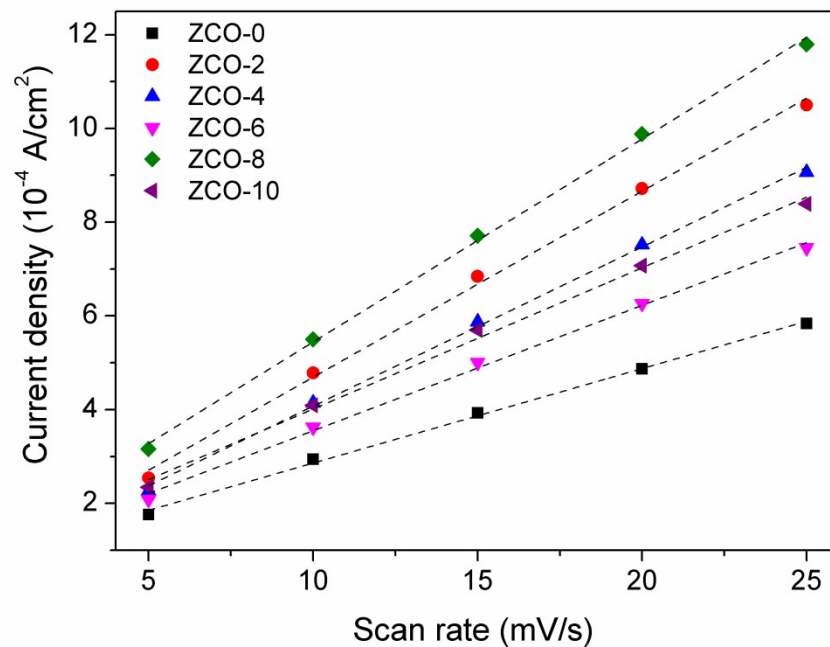


Fig. S5. Capacitive current density as a function of scan rate of $Zn_xCo_{3-x}O_4$

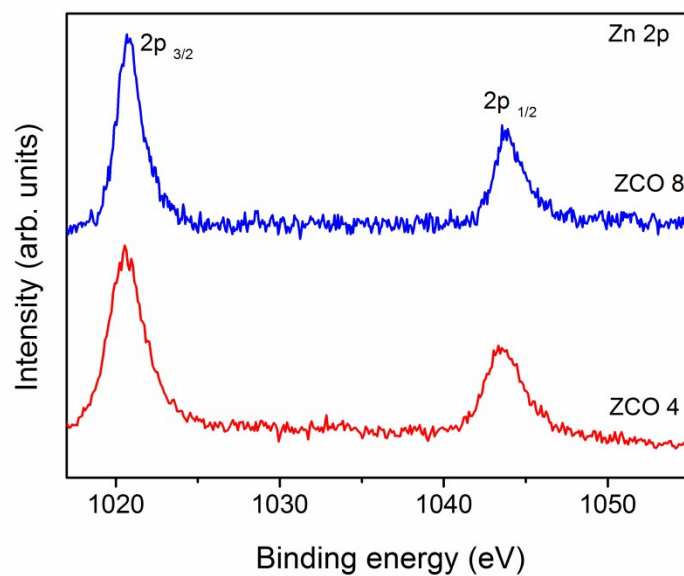


Fig. S6. Zn 2p XPS spectra of $Zn_xCo_{3-x}O_4$

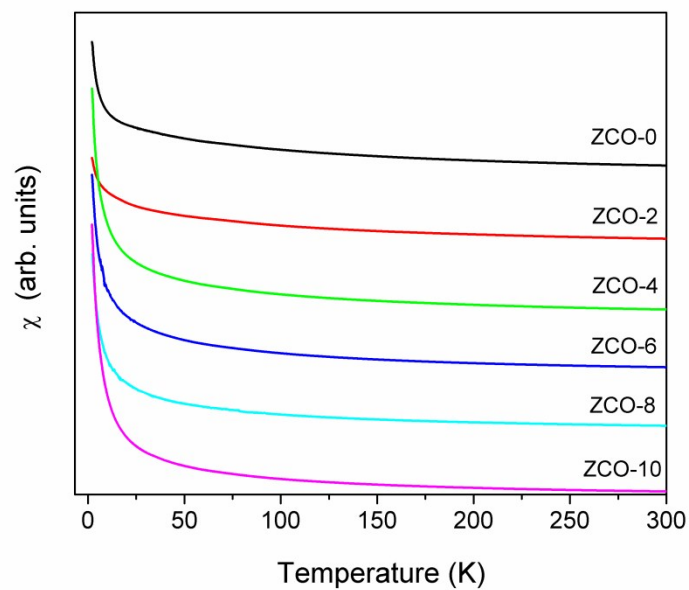


Fig. S7. DC magnetic susceptibility curves of $\text{Zn}_x\text{Co}_{3-x}\text{O}_4$. The curves are shifted along the y -axis.

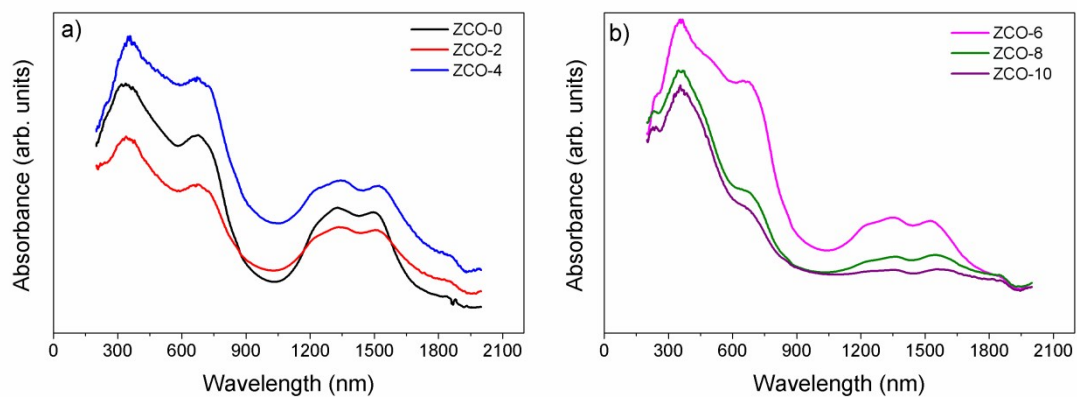


Fig. S8. (a,b) Electronic absorption spectra of $\text{Zn}_x\text{Co}_{3-x}\text{O}_4$ without baseline correction

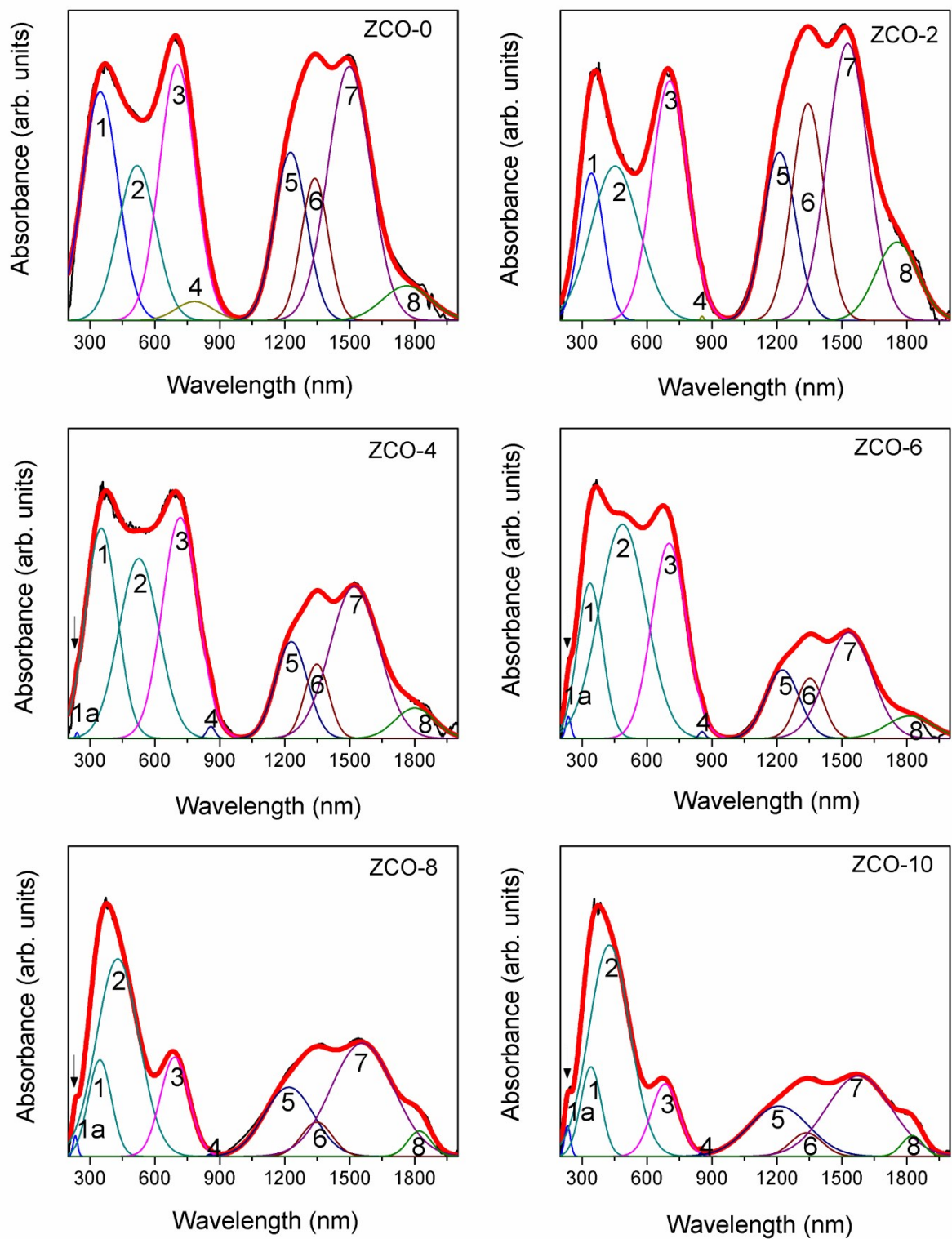


Fig. S9. Deconvoluted absorption spectra of $Zn_xCo_{3-x}O_4$ (peak-1a is present only from $x=0.4$ to $x=1$ in $Zn_xCo_{3-x}O_4$ and it is indicated by the arrow mark).

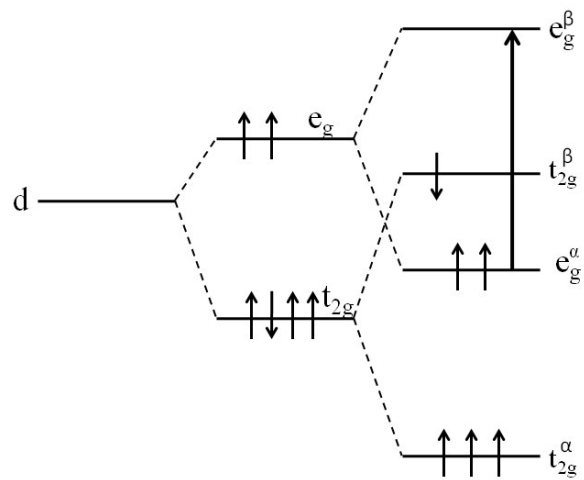


Fig. S10. 3d-energy levels splitting of high spin Co^{3+} [1]

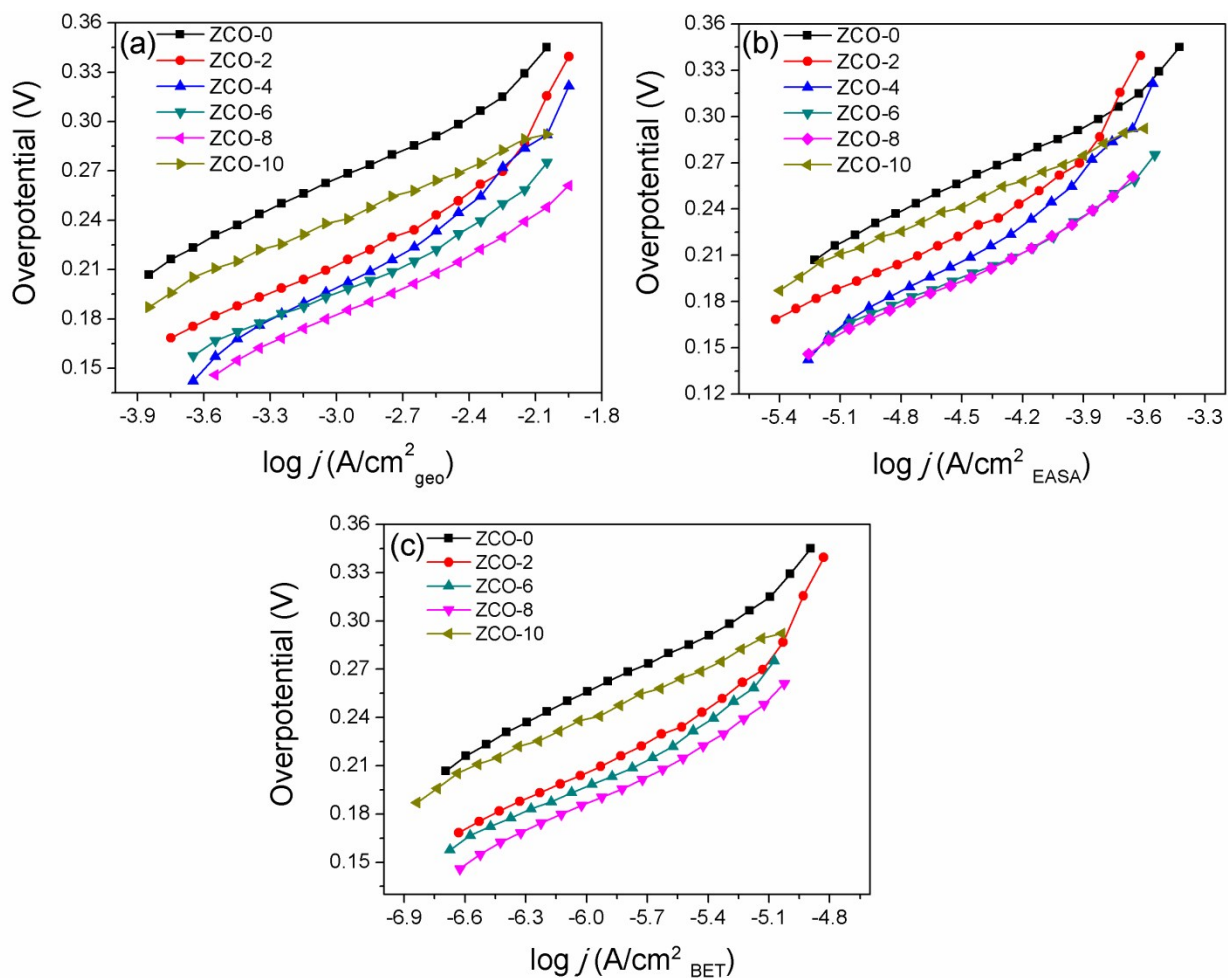


Fig. S11 Tafel plots of OER activities of Zn_xCo_{3-x}O₄ normalized by (a) geometrical surface area of the electrode, (b) electrochemically active surface area (EASA), and (c) Brunauer-Emmett-Teller (BET) surface area.

Table S1. Lattice parameter and crystallite size of $Zn_xCo_{3-x}O_4$

Sample code	Composition	Lattice parameter a (Å)	Crystallite size (±1 nm)
ZCO-0	Co_3O_4	8.075	7
ZCO-2	$Zn_{0.2}Co_{2.8}O_4$	8.090	6
ZCO-4	$Zn_{0.4}Co_{2.6}O_4$	8.084	11
ZCO-6	$Zn_{0.6}Co_{2.4}O_4$	8.108	12
ZCO-8	$Zn_{0.8}Co_{2.2}O_4$	8.116	10
ZCO-10	$ZnCo_2O_4$	8.143	11

Table S2. Elemental composition from EDX

Sample code	Composition	Theoretical Zn/Co ratio	Experimental Zn/Co ratio from
ZCO-2	$Zn_{0.2}Co_{2.8}O_4$	0.0714	0.0720
ZCO-4	$Zn_{0.4}Co_{2.6}O_4$	0.1538	0.1515
ZCO-6	$Zn_{0.6}Co_{2.4}O_4$	0.2500	0.2587
ZCO-8	$Zn_{0.8}Co_{2.2}O_4$	0.3636	0.3631

Table S3. Comparisons of the ratios of Co^{2+}/Co^{3+} obtained from the XPS spectra

Sample name	Co^{2+}/Co^{3+}	Expected ratio
ZCO-0 (Co_3O_4)	0.49	0.5
ZCO-4 ($Zn_{0.4}Co_{2.6}O_4$)	0.31	0.3
ZCO-8 ($Zn_{0.8}Co_{2.2}O_4$)	0.11	0.1

Table S4. Curie constant and spin values of $Zn_xCo_{3-x}O_4$ from the magnetic studies.

Sample code	Curie constant (emu K mol ⁻¹)	Total spin	Spin contribution from Co ³⁺
ZCO-0	2.87	1.94	0.45
ZCO-2	2.48	1.79	0.59
ZCO-4	2.20	1.66	0.77
ZCO-6	2.05	1.58	0.99
ZCO-8	1.55	1.34	1.04
ZCO-10	1.58	1.35	1.35

Table S5. Assignments of the transitions for the deconvoluted peaks in the absorption spectra of $Zn_xCo_{3-x}O_4$. The references in the brackets refer to the references in the main manuscript.

No	Energy of the bands		Transition	References
	in eV	in nm		
Peak 1	3.70 – 3.46	334-359	LMCT O ²⁻ → Co ²⁺	2 [47]
Peak 1a	5.17-5.33	233-240	LMCT O ²⁻ → Zn ²⁺	3,4 [50,51]
Peak 2	2.77 – 2.44	446- 506	Co ³⁺ (H.S) d-d $\sigma^* e_g^\alpha \rightarrow \sigma^* e_g^\beta Co$	1 [52]
Peak 3	1.8 – 1.75	691.5 – 709.4	$t_{2g}(Co^{3+}) \rightarrow t_2(Co^{2+})$	5 [48]
Peak 4	1.47 – 1.44	844 – 863	Due to some electronic defects by oxygen vacancies	2 [47]
Peak 5	1 -1.02	1232 - 1219	Co ²⁺ $\pi^2 t_2 \rightarrow Co^{3+} \sigma^* e$	5 [48]
Peak 6	0.925 - 0.912	1339.3 – 1360	Co ²⁺ → $e_g^* Co^{3+}$	5 [48]
Peak 7	0.825 - 0.78	1503 - 1588	Co ²⁺ $\pi^* e \rightarrow \pi^* t_2$	5 [48]

Table S6. BET surface area of $Zn_xCo_{3-x}O_4$

Sample code	BET surface area (m ² /g)
ZCO-0	70
ZCO-2	76
ZCO-6	106
ZCO-8	119
ZCO-10	97

Table S7. Overpotential values of $Zn_xCo_{3-x}O_4$ based on the current density normalized by geometrical surface area, electrochemically active surface area (EASA) and Brunauer–Emmett–Teller (BET) surface area, calculated from Fig. S11

Sample code	Overpotential (mV) at 1.0×10^{-2} A/cm ² (Geometrical surface area)	Overpotential (mV) at 1.0×10^{-4} A/cm ² (EASA)	Overpotential (mV) at 6.3×10^{-6} A/cm ² (BET surface area)
ZCO-0	358	287	307
ZCO-2	325	264	264
ZCO-4	306	250	-
ZCO-6	287	226	256
ZCO-8	254	226	241
ZCO-10	300	270	285

References:

1. I. D. Belova, Y. E. Roginskaya, R. R. Shifrina, S. G. Gagarin, Y. V. Plekhanov and Y. N. Venevtsev, *Solid State Commun.*, 1983, **47**, 577-584.
2. M. Lenglet and C. K. Jørgensen, *Chem. Phys. Lett.*, 1994, **229**, 616-620.

3. S. K. Sampath and J. F. Cordaro, *J. Am. Ceram. Soc.*, 1998, 81, 649-654.
4. C. R. Mariappan, R. Kumar and G. V. Prakash, *RSC Adv.*, 2015, 5, 26843-26849.
K. Miedzinska, B. Hollebone and J. Cook, *J. Phys. Chem. Solids*, 1987, **48**, 649-656.